

Semicircular Canals Input Can Modify the Fast-Phase Nystagmus in Off-Vertical Axis Rotation of Mice

Shijie Xiao,^{1*}  Tong Zhao,^{1*} Wenda Liu,² Zihao Peng,² and Fangyi Chen¹

¹Department of Biomedical Engineering, Southern University of Science and Technology, Shenzhen 518055, China and ²Giant Technologies Co., Ltd, Shenzhen 518055, China

Abstract

Vestibular research is essential for understanding and treating disorders such as vertigo and Meniere's disease. The vestibulo-ocular reflex (VOR) is a key method for assessing vestibular function and an essential tool for diagnosing vertigo. Traditionally, the VOR comprises angular VOR (aVOR) and translational VOR (tVOR), which originate from the vestibular semicircular canals (SCCs) and otolith organs, respectively. VOR consists of both fast-phase and slow-phase eye movements, which functionally interact to contribute to gaze control. However, to calculate the gain and phase parameters of the VOR, it is common practice to exclude fast-phase information superimposed on slow-phase eye movements. As a result, the information contained in the fast phase has not been fully utilized. OVAR is primarily used to evaluate otolith function, as there is no SCC input during its steady state. It is widely accepted that fast-phase nystagmus (FPN) during OVAR is generated by periodic otolith inputs via the central vestibular velocity storage mechanism. Surprisingly, we discovered in this study that SCC input can modify the generation of FPN in mouse OVAR test, as demonstrated by testing *Zpld1* (Zona pellucida-like domain containing 1 protein) mutant mice with SCC deficits. This finding was further confirmed using both unilateral and bilateral semicircular canals dehiscence surgical models. In addition to revealing the dependence of FPN on SCC input, we demonstrated that FPN can be used to evaluate vestibular function, particularly in conditions that are difficult to assess using slow-phase eye movements, such as unilateral vestibular lesions and central modulation via baclofen treatment.

Key words: fast-phase nystagmus; off-vertical axis rotation; slow-phase nystagmus; unilateral vestibular lesion; vestibular ocular reflex; vestibular organ

Significance Statement

Although the vestibular semicircular canal (SCC) input is absent during the steady state of OVAR test, we discovered that SCC input can modify the generation of fast-phase nystagmus (FPN) in mice. This was demonstrated using *Zpld1* mutant mice with SCC deficits and further confirmed through semicircular canal dehiscence models. Additionally, we found that FPN is valuable for assessing vestibular function in conditions such as unilateral vestibular lesions and in cases of central modulation by baclofen, making it a promising diagnostic tool for vestibular clinics.

Introduction

Vestibular research is essential for understanding and treating disorders such as vertigo, Meniere's disease, and vestibular migraines, which are prevalent in aging populations and increase the risk of falls (Osoba et al., 2019). It also plays a key role in space exploration and addresses vertigo and vomiting induced by virtual reality (Ng et al., 2020; Hupfeld et al., 2022). In recent years, mice have become the predominant model in inner ear research and are widely used in studies on vestibular toxicity (Zeng et al., 2020; Gao et al., 2022), development (Burns and Stone, 2017), genetics

Received Oct. 25, 2024; revised Feb. 6, 2025; accepted Feb. 12, 2025.

The authors declare no competing financial interests.

Author contributions: S.X., T.Z., and F.C. designed research; S.X., T.Z., W.L., and Z.P. performed research; S.X. and T.Z. contributed unpublished reagents/analytic tools; S.X. analyzed data; S.X. and F.C. wrote the paper.

This work was supported by the National Key R&D Program of China (grant numbers 2023YFF1203505, 2024YFC2417900), Shenzhen Science and Technology Program (grant number KJZD20230923114909019) and Shenzhen Municipal Science and Technology Innovation Council (grant number 202110293000007).

*S.X. and T.Z. contributed equally to this work.

Correspondence should be addressed to Fangyi Chen at chenfy@sustech.edu.cn.

Copyright © 2025 Xiao et al.
This is an open-access article distributed under the terms of the [Creative Commons Attribution 4.0 International license](https://creativecommons.org/licenses/by/4.0/), which permits unrestricted use, distribution and reproduction in any medium provided that the original work is properly attributed.

(Armstrong et al., 2015; Vijayakumar et al., 2019; Simon et al., 2021), and function. Vestibular function is a crucial indicator for understanding and monitoring the physiological state of the vestibular system, highlighting the urgent need for effective vestibular function assessments in these research areas. The vestibulo-ocular reflex (VOR) originates from the peripheral vestibular end organs including vestibular semicircular canals (SCCs) and otolith organs and transmits signals to the extraocular muscles through a direct or relatively direct pathway in the brainstem (Katsarkas et al., 1991), where head velocity information is converted into appropriate oculomotor signals (Katsarkas et al., 1991). Furthermore, the VOR is also modulated by the central nervous system to facilitate vestibular compensation or adaptation. Recently, with the development of both customized (Nist-Lund et al., 2019; Ono et al., 2020) and commercially available VOR test systems (Yang et al., 2020), mouse VOR tests have gradually surpassed the previously prevalent method of vestibular sensory evoked potentials (VsEP) and have become more popular in various laboratories.

It is important to note that, VOR contains both fast-phase and slow-phase eye movements (Furman, 2010), which interact to contribute to gaze control. However, to calculate the gain and phase parameters of the VOR, it is common practice to exclude fast-phase information superimposed on the slow-phase eye movements (Ebisawa et al., 1988; Ranjbaran et al., 2016; Kim et al., 2021), leaving the information in fast-phase nystagmus (FPN) underutilized (Katsarkas et al., 1991; Furman, 2010). Slow-phase eye movement is determined by the direct pathway of the angular VOR (aVOR) or the relatively direct pathway of the translational VOR (tVOR; Shimizu et al., 2016), and thus its features (gain and phase) are insufficient to reflect many subtle but important vestibular deficits involving the central pathway. In contrast, the generation of FPN depends on both direct and central pathways. Experiments have demonstrated that FPN is related to central VSM (Laurens and Angelaki, 2011; Shimizu et al., 2016), a regulatory mechanism involving the vestibular cerebellum, which is primarily responsible for establishing multisensory rotation signals (Laurens and Angelaki, 2011). Since both peripheral and central systems are involved in generating FPN, abnormal sensory signal processing can arise from either central or peripheral vestibular inputs (Choi et al., 2007). Therefore, efficiently utilizing FPN may be beneficial for detecting vestibular deficits, especially those that are undetectable by slow-phase eye movements. Furthermore, FPN in vision-induced eye movement has been used to study the central nervous system disorders (Kanayama et al., 1987) and the effect of psychiatric drugs (Wang et al., 2005). FPN in aVOR has been used to determine the lesion side in unilateral vestibular lesion (UVL; Curthoys, 2002). Thus, studying FPN not only helps in understanding the central integration of peripheral inputs but also in discovering new clinical applications.

The aVOR and OVAR are commonly used in clinical and animal experiments to assess the functionality of the vestibular peripheral SCCs (Beraneck and Cullen, 2007; Fetter, 2007) and otolith organs (Brettler et al., 2000; Maruta et al., 2001), respectively. In aVOR mode, sinusoidal yaw oscillation primarily stimulates the horizontal SCCs (H-SCCs). In contrast, during OVAR mode, constant speed rotation along a tilted axis results in continuous changes in head orientation relative to gravity. Eye movements during OVAR are complex, involving horizontal, vertical, and torsional components. During the steady state of OVAR, the input from SCCs ceases, and eye movements are primarily driven by otolith signals. Vertical and torsional sinusoidal modulation components (SMC) are mainly utilized for evaluating changes in vestibular function due to otolith stimulation along the interaural and naso-occipital axes (Angelaki and Hess, 1996). The horizontal SMC (H-SMC) is small and can be isolated by eliminating the strong FPN.

In this study, we investigated the horizontal FPN (H-FPN) in OVAR. Several reasons guided our focus on H-FPN in OVAR: (1) it reflects both central and peripheral conditions of the vestibular system; (2) H-FPN was prominent in horizontal eye movement in mouse OVAR test, an aspect that is often underutilized in the analysis of results. During our investigation of this overlooked feature, we found that the input from SCCs can modify the generation of H-FPN in mouse OVAR test, consistent with findings from primate studies. Moreover, H-FPN is sensitive to various vestibular deficits, highlighting its potential as a diagnostic tool in vestibular clinics.

We developed a four-channel mouse pseudo-OVAR (pOVAR) testing system based on the principle of eccentric counter-rotation (CR; Kaufman, 2002; Shimizu et al., 2015). This dual-axis setup generates separate or combined stimuli to the SCCs and otolith organs. Eccentric axis movement provides angular acceleration stimulation, while the main axis rotation applies linear force stimulation. When both axes rotate at a constant velocity, the system simulates the tilted rotation modes of OVAR. The FPN in the horizontal eye movements during this pOVAR stimulation was extracted to assess the vestibular dysfunction.

The system was validated using three vestibular deficit mouse models: (1) IDPN, a commonly used vestibular toxicant (Khan et al., 2009), which causes loss of inner ear hair cells in rodents, leading to irreversible damage to the peripheral vestibular system (Wilkerson et al., 2018; Zeng et al., 2020). IDPN is frequently employed in studies of inner ear hair cell regeneration. (2) Baclofen, a vertigo-control drug, acts as an agonist of gamma-aminobutyric acid type B (GABA_B) receptors (Dai et al., 2006; Ebenezer and Prabhaker, 2007; Shimizu et al., 2016). GABA is a major neurotransmitter involved in the VSM, and baclofen can inhibit neuronal activity in this network, affecting vestibular function. Both drugs were administered intraperitoneally at various concentrations. The results demonstrated a strong correlation between FPN frequency and drug concentration. (3) UVL, a common model in vestibular research, simulates clinical conditions such as vestibular neuritis (Fetter, 2016) to study compensation and adaptation in the vestibular system (Sadeghi et al., 2011; Hubner et al., 2017; Khan et al., 2022). A critical challenge in UVL models is identifying the side of the lesion. During the early stages, the aVOR slow-phase eye movements are asymmetrical to the lesion side but gradually becomes symmetrical due to the central compensation of asymmetrical inhibition after ~1–2 weeks. Although it is claimed that asymmetrical slow-phase

aVOR can be detected (Beraneck et al., 2008; Hubner et al., 2017), results are often inconclusive, and it is generally accepted that the lesion side cannot be identified from slow-phase eye movements due to the bilateral vestibular “push–pull” mechanism and the strong compensatory ability of the vestibular system (Fetter, 2016). However, FPN, which involves the central pathways, can reflect asymmetrical inhibition by the central vestibular system. We demonstrated asymmetrical FPN frequency toward and away from the lesion side in UVL models.

The most intriguing finding was that mice with bilateral horizontal semicircular canal damage failed to produce FPN in the OVAR test. The *Zpld1*^{−/−} mouse, which has impaired canal function but normal otolith function, exhibited a normal vertical SMC (V-SMC) during OVAR. However, the horizontal H-FPN was nearly absent, consistent with the OVAR results in monkeys that underwent bilateral H-SCC neurectomy. This finding was confirmed in both unilateral and bilateral semicircular canals dehiscence (SCD) models. The V-SMC was normal in unilateral SCD mice and mildly impaired in bilateral SCD mice, but H-FPN was significantly reduced in both cases. These results indicate that SCC inputs may modify the generation of H-FPN in the mouse OVAR test.

In addition to this discovery, with this system, experimental results demonstrated the advantage of utilizing FPN in effectively identifying various subtle vestibular deficits, especially those undetectable with traditional V-SMC in OVAR. Moreover, the structure can accommodate multiple eccentric rotation platforms within the same main rotation circle, thus enhancing spatial efficiency for constructing a high-throughput system.

Materials and Methods

The four-channel dual-axis mouse VOR test system

The diagram of the four-channel mouse VOR test system is shown in Figure 1A. Testing parameters (main and eccentric axis rotation velocity, direction, duration, etc.) can be programmed into a motor controller to manipulate the main and eccentric axis motor movement, thereby performing corresponding vestibular stimulation. The centers of the mouse binaural coincide with the center of rotation of the eccentric axis, ensuring alignment between the vestibular system and the rotation axis. Simultaneously, two infrared motion cameras (EZVIZ S6, China) record the eye movement trajectories of mice, with the videos transmitted to a computer via Wi-Fi for subsequent analysis.

The pOVAR modes were used in this study. In the conventional OVAR mode, the animal is tilted relative to the horizontal plane, generating roll and pitch of the head while rotating the platform, as shown in Figure 1B. In pOVAR mode, this tilt is simulated by the centrifugal force relative to the Earth's vertical axis, generated by the main axis rotation. The angle θ represents the angle of resultant gravity-centrifugal force relative to the Earth's vertical axis, equivalent to the tilt in the classic OVAR test. The magnitude of the simulated tilt angle θ is determined by the main axis rotation velocity and radius, considering a constant gravity of 1 g. For a fixed radius of 17 cm in our setup, the main axis velocities $V_M = 186, 264, 336, 408^\circ/\text{s}$ simulates tilt angle $\theta = 10^\circ, 20^\circ, 30^\circ, 40^\circ$ in a conventional OVAR test. Meanwhile, the eccentric axis rotation velocity determines the modulation frequency of the linear acceleration ($V_E = 36, 72, 108, 144^\circ/\text{s}$ corresponds to frequency $f = 0.1, 0.2, 0.3, 0.4$ Hz). During steady-state operation of the system, the direction of the mouse VOR is related only to the direction of the eccentric axis rotation and is independent of the direction main axis movement.

Stimulus protocols

The experiments were conducted in complete darkness to avoid visual interference. Mice were treated with 2% pilocarpine 10 min before the experiment to prevent pupil dilation in darkness. To thoroughly investigate the characteristics of the mouse vestibular system, two different rotation paradigms were employed.

pOVAR mode for testing otolith organs. Both the main and eccentric axis rotate simultaneously at their own constant velocity and four mice can be tested simultaneously (Fig. 1C). Two different rotation paradigms were performed during pOVAR: (1) at fixed main axis velocity ($336^\circ/\text{s} = 30^\circ$) with different rotational velocity of eccentric axis ($72, 108, 144^\circ/\text{s} = 0.2, 0.3, 0.4$ Hz) and (2) at fixed eccentric axis velocity ($72^\circ/\text{s} = 0.2$ Hz) with different main axis velocity ($186, 264, 336, 408^\circ/\text{s} = 10^\circ, 20^\circ, 30^\circ, 40^\circ$). The rotational direction (CW or CCW) of the two axis was set according to the experimental needs (Fig. 3). To obtain sufficient eye movement information, a 3 min video was recorded under each parameter condition, with at least a 1 min interval between different parameter experiments. The evoked V-SMC was used to evaluate the otolith dysfunction. More interestingly, the FPN was used to show the contribution of the SCCs to this conventional otolith measurement method.

Animals

All animal care procedures and experimental protocols described in this paper were approved by the Animal Care and Ethics Committee of the Southern University of Science and Technology. Mice were housed under 12 h light/dark cycling conditions with *ad libitum* access to water and food. The experiments involved both genders at 6–8 weeks of age, each weighing ~20 g. Three mouse models, IDPN, baclofen, and UVL, were used to validate the system and demonstrate the potential of FPN in evaluating subtle vestibular deficits. Two genetic models, *zpld1* and *otop1* (Otopetrin1) mice, along with unilateral and bilateral SCD mice, were used to investigate the impact of the semicircular canal (SCC) on the generation of H-FPN during pOVAR.

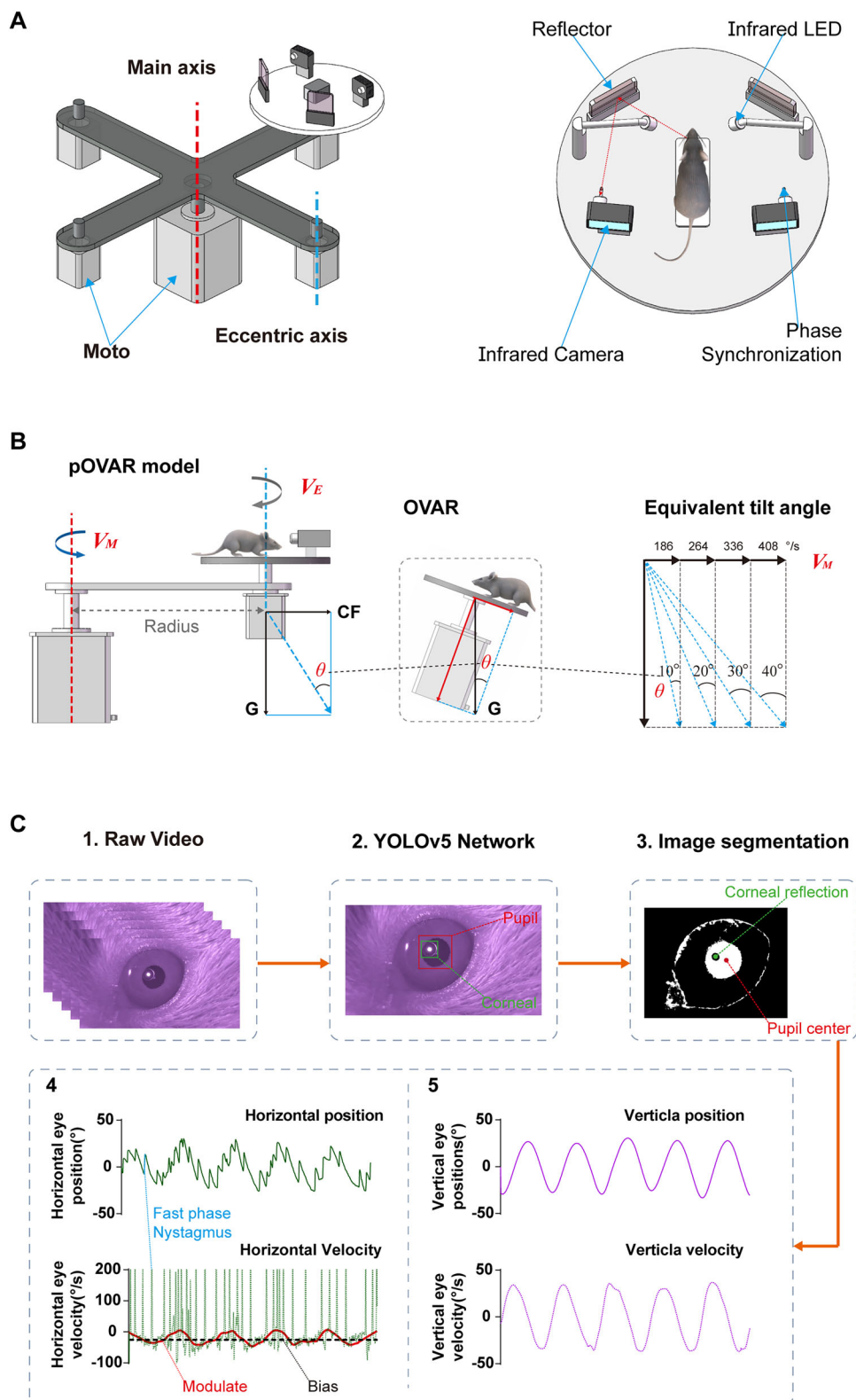


Figure 1. Four-channel mouse VOR test system. **A**, Left, The schematic of four-channel system with one main axis (dashed red line) and four eccentric axes (dashed blue line). Right, Layout diagram of the turntable at the eccentric axis. Two infrared motion cameras are mounted on micromanoeuver platforms and record mouse eye movements via mirrors (dashed red line). The LED in front of the camera emits light for 10 ms when the turntable starts, which is used to calculate the VOR phase. **B**, The pOVAR test mode. **C**, Mouse eye movement video processing flowchart. CW, clockwise; CCW, counter clockwise; V_M , main axis velocity; V_E , eccentric axis velocity; G, gravity; CF, centrifugal force.

Vestibulo-toxicity—IDPN administration. 3,3'-Iminodipropionitrile (IDPN, TCI, I0010) was dissolved in physiological saline solution. Eighteen C57BL/6J wild-type mice were used for the vestibulotoxic drug study and divided into two experimental groups and one control group. Mice in the two experimental groups were injected intraperitoneally with IDPN at doses of 2 and 4 mg/g ($\approx 4 \mu\text{l/g}$), respectively. Mice in the control group received the same volume of saline solution ($4 \mu\text{l/g}$). The pOVAR test was conducted before and after IDPN injection (Fig. 2A–D).

Central vestibular manipulation—baclofen administration. Systemic administration of baclofen specifically inhibits VSM activity and decreases susceptibility to motion sickness (Dai et al., 2006; Cohen et al., 2008). Baclofen was purchased from MedChemExpress (MCE, HY-B0007) and dissolved in physiological saline solution. Fifteen C57BL/6J wild-type mice were divided into three groups: two experimental and one control. The experimental group mice received intraperitoneal injections of baclofen at a dosage of 5 and 10 mg/kg. Control group mice were injected with saline. The pOVAR test was conducted before and 90 min after drug administration. The dosage and administration route were based on previous studies (Ebenezer and Prabhaker, 2007; Shimizu et al., 2016).

Unilateral vestibular lesion. Surgical procedures for unilateral creating vestibular peripheral lesions and postoperative care are based on previously published methods (Guo et al., 2017, 2018). First, an adult mouse was anesthetized via intraperitoneal injection of dexmedetomidine hydrochloride injection (Dexdomitor, 0.08 mg/kg) and Zoletil 50 (32 mg/kg), while meloxicam (1 mg/kg) was administered subcutaneously for analgesia. Next, the skin of mouse's head was disinfected with 75% ethanol, and an incision was made along the retroauricular groove to expose the lateral semicircular canal (LSC) and the posterior semicircular canal (PSC). A small hole was drilled in the middle of the LSC using a 26 G needle, allowing endolymph to leak. The hole was then enlarged slightly beyond the diameter of the injection cannula. The cannula was inserted ~ 2 mm into the LSC toward the ampulla, and $15 \mu\text{l}$ of gentamycin (MACKLIN, G810322, 8 mg/ml) was injected using a microsyringe pump (TJ-2A). After the injection, the LSC hole was sealed with a small piece of muscle.

Unilateral and bilateral semicircular canals dehiscence. Injection of gentamicin through the semicircular canal can lead to damage to both the unilateral semicircular canal and the otolith organs. In contrast, the SCD technique selectively damages the semicircular canal while preserving the function of the otolith organs. Following the procedure for UVL, the SCD involves drilling a hole in the middle of the LSC, absorbing the leaking endolymphatic fluid with sterile cotton, and leaving the LSC hole unsealed. Performing unilateral or bilateral SCD surgery allows selective damage to the respective semicircular canals while preserving otolith function.

To account for surgical variability and individual differences in vestibular system performance, we increased the number of experimental mice to reduce error. Twenty-eight C57BL/6J wild-type mice were divided into three groups: 8 served as controls, 10 underwent left-UVL, and 10 underwent right-UVL. Mice were allowed 10 d to recover postoperatively, and the pOVAR test was conducted before and after surgery.

Mice with genetic deficits in SCC and otolith organ

Otop1 and *Zpld1* mutant mice were used for validating the system performance in localizing vestibular organ dysfunction. The *Zpld1* mouse was also used to investigate the necessity of SCC input for the H-FPN in the pOVAR test mode. The spontaneous recessive mutation in the *Otop1* gene, located on chromosome 5, alters the pH of the inner ear, preventing the development of otolith particles composed of calcium carbonate crystals (Hurle et al., 2003). Consequently, *Otop1*^{tit/tit} mice exhibit abnormal otolith function, while the SCCs remain unaffected. In contrast, *Zpld1*^{-/-} mice exhibit impaired SCC function but normal otolith function. The *Zpld1* gene is primarily expressed in ampullary crista cells, and the *Zpld1* protein is a major component of the mouse cupula (Vijayakumar et al., 2019). Groups of five animals were used in each mutant group, with an additional wild-type group serving as a control.

Data analysis

Pupil tracking. In this study, we employed a deep learning-based target recognition algorithm for pupil tracking. On this basis, threshold segmentation was applied, as depicted in Figure 1C. Each frame of the eye movement video was first processed through a pretrained YOLOv5 model to detect the pupil. The region containing the pupil was then cropped based on the predicted bounding box. Next, threshold segmentation was applied to convert the cropped image into a binary format. Finally, an ellipse-fitting algorithm was used to delineate the pupil contour, accurately determining the pupil's center. This method enabled precise tracking of the mouse pupil's displacement in both horizontal and vertical directions (Fig. 1C4,C5).

Fast-phase nystagmus extraction. In the pOVAR test, horizontal eye movements exhibit both FPN and SMC (Fig. 1C4), with their direction closely correlated to the motion of the eccentric axis. We implemented an algorithm from a previous study (Behrens and Weiss, 1992) to separate the fast phases and slow phases. First, the displacement data were processed using a low-pass filter to eliminate minor high-frequency vibrations. Subsequently, a second-order differentiation was applied to obtain the absolute acceleration values. FPN was identified in the time domain by applying appropriate

thresholds, allowing for the separation of the fast and slow phases. Finally, the FPN frequency was calculated. Typically, we selected eye-tracking data collected 1 min after the device startup for analysis.

Results

The effects of peripheral (IDPN) and central disorder (baclofen) on FPN and sinusoidal modulation component in pOVAR test

The V-SMC during the pOVAR test on Day 9 after IDPN administration is shown in [Figure 2A,B](#). The control group exhibited significantly larger displacement than both the mid-dose and high-dose groups across all tilt angles. Eye displacement in the mid-dose group (2 mg/g) was higher than that in the high-dose group (4 mg/g). The H-FPN frequency also displayed varying degrees of attenuation, but with considerable individual differences within groups, as shown in [Figure 2C,D](#) (two-way ANOVA). The horizontal mean slow-phase velocity/bias velocity was similar to the H-FPN frequency, as shown in [Figure 2E](#) (two-way ANOVA). These findings suggest that intraperitoneal IDPN injection damages the peripheral vestibular structures in mice. While SMC can be used for a quantitative assessment of vestibular dysfunction severity, H-FPN/bias velocity is also capable of quantifying vestibular damage, albeit with greater error than SMC, reflecting the complexity of FPN. Baclofen administration (5 and 10 mg/kg) had little effect on the modulation component during the pOVAR test ([Fig. 2G,H](#)), though the H-FPN frequency was reduced ([Fig. 2E](#)). Compared with the control group, the H-FPN frequency in the baclofen-treated groups was significantly reduced, with a more pronounced decrease in the high-dose (10 mg/kg) group ([Fig. 2F](#), one-way ANOVA).

UVL mice exhibit asymmetric FPN frequency in pOVAR test

During the pOVAR test on mice, the direction of the eccentric axis rotation was alternated (from CCW to CW) and kept opposite to the main axis rotation. Compared with the control group, V-SMC in the surgery group was significantly reduced in both CCW and CW directions. However, no significant difference was observed between the right-UVL and left-UVL groups. Additionally, no differences in V-SMC between the left and right eyes were detected under either CCW or CW stimulation conditions ([Fig. 3F](#), two-way ANOVA). These results indicate that UVL surgery attenuates overall vestibular performance. However, using SMC data alone in the pOVAR test could not distinguish whether the injury occurred on the right or left side.

In contrast, the H-FPN frequency in left-UVL mice was significantly lower in the CCW direction than in the CW direction, while the opposite was true for right-UVL mice. No difference in H-FPN frequency between CCW and CW directions was detected in the control group ([Fig. 3A–E](#); Extended Data [Fig. 3-1D–I](#), two-way ANOVA). The normalized results are shown in [Figure 3E](#). In the control group, the ratio of CW to CCW was ~ 1 , while in the surgery groups, the ratio was significantly < 1 , with the right-UVL group showing a more pronounced difference than the left-UVL group (one-way ANOVA). The V-SMC and H-FPN frequency under other stimulus conditions are shown in Extended Data [Figure 3-1](#).

For mice with L-SCD and intact otolith function, V-SMC in the pOVAR test did not show significant differences compared with normal mice ([Fig. 3G](#), Extended Data [Fig. 3-1J](#)). However, the H-FPN frequency also exhibited significant asymmetry ([Fig. 3H,I](#); Extended Data [Fig. 3-1K,L](#), two-way ANOVA). Therefore, the lesion side in UVL could be identified based on H-FPN, with the potential mechanism discussed in the discussion section.

Furthermore, the FPN of UVL mice exhibited a distinct bias in aVOR test ([Fig. 4A](#)). During rotation toward the healthy side, normal FPN appeared; however, when rotating toward the injury side, the FPN significantly diminished or even ceased entirely ([Fig. 4B,C](#)). For slow-phase eye movements in the aVOR test, within certain limits, the bilateral H-SCCs generate symmetrical “push–pull” signals via the abducens nucleus and oculomotor nucleus, resulting in coordinated slow-phase movements ([Fig. 4D](#)). In contrast, the generation of FPN primarily relies on unilateral excitatory vestibular input, as shown in [Figure 4E](#) (Curthoys, 2002), thereby resulting in the bias of FPN.

FPN reflects conditions on the SCC even in a traditional otolith testing mode

The *Otop1^{ttt/ttt}* mice with otolithic dysfunction exhibited almost no VOR during the steady state of pOVAR test ([Fig. 5A–C](#)). However, at the onset and cessation of the test, nystagmus characterized by alternating fast and slow phases was observed due to the activity of the SCCs and VSM in the trapezoidal angular velocity (TAV) model ([Fig. 5D](#)). The stimulus paradigm of the TAV model was illustrated in Extended Data [Figure 5-1F](#). *Otop1^{ttt/ttt}* mice exhibited normal vestibular time constants, indicating the intact function of the SCCs and VSM. In contrast, *Zpld1^{-/-}* mice demonstrated significant impairment in VSM function ([Fig. 5E](#)). The V-SMC results showed no difference between *Zpld1^{-/-}* and WT mice under all stimulus conditions, indicating normal otolith function in *Zpld1^{-/-}* mice ([Fig. 5B,C](#); Extended Data [Fig. 5-1B](#), two-way ANOVA). In contrast, there were significant differences in the horizontal fast-phase component, with *Zpld1^{-/-}* mice lacking H-FPN ([Fig. 5F,G](#); Extended Data [Fig. 5-1A](#), two-way ANOVA). Bilateral L-SCD surgery in mice resulted in inactivation of the H-SCCs, a significant decrease in VOR gain value, and a slight impairment of otolith function ([Fig. 5H,I](#); Extended Data [Fig. 5-1C,D](#), two-way ANOVA). Due to surgical variability, some mice retained higher levels of SCC function, as indicated by the red triangles in [Figure 5H,J](#). Notably, bilateral H-SCCs dysfunction led to a significant reduction in H-FPN during the

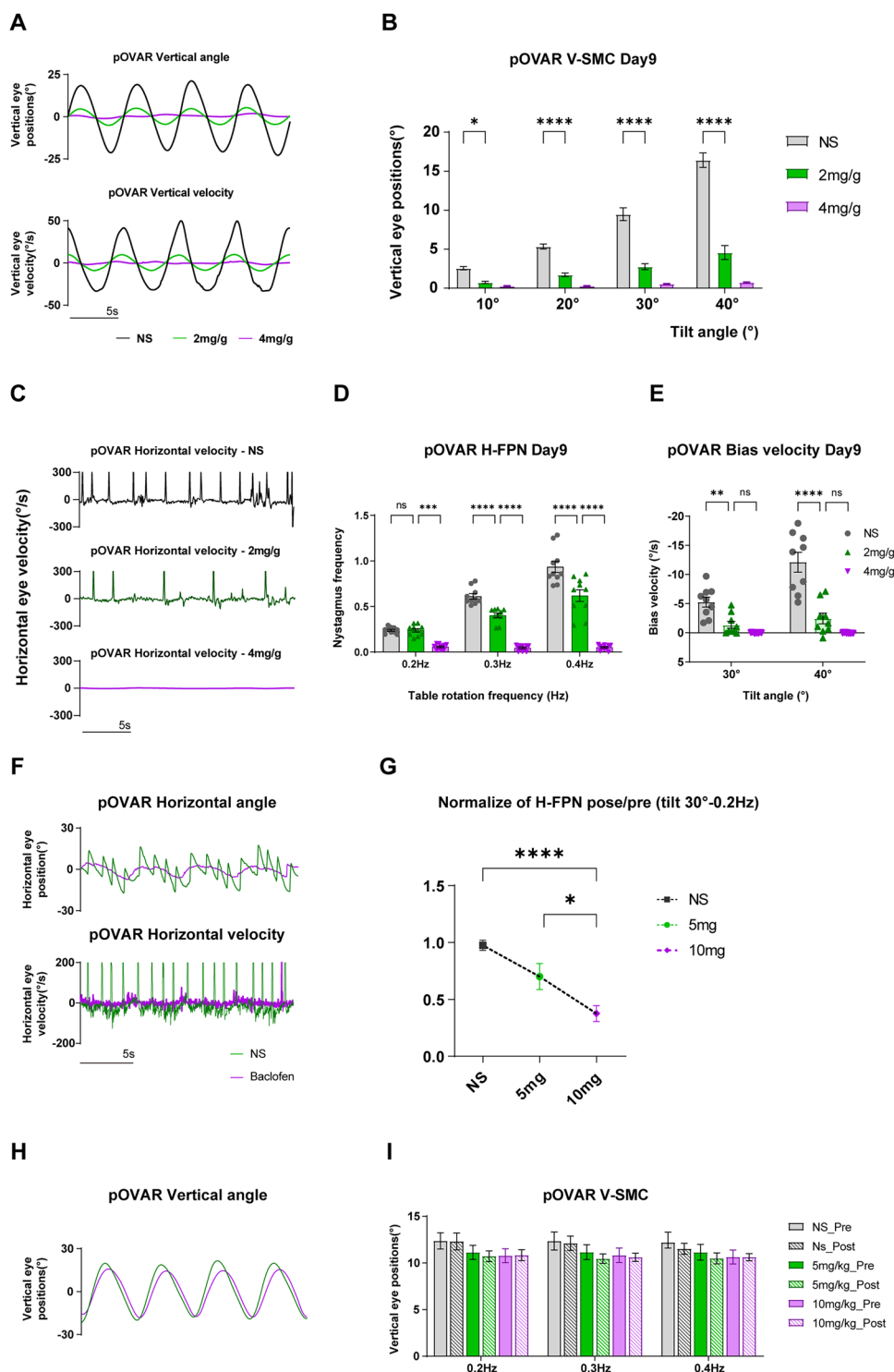


Figure 2. Effect of IDPN and baclofen on mouse vestibular function. Means \pm standard error of mean (SEM) is shown in the Results. **A**, Traces display vertical eye displacement and velocity in mice. **B**, V-SMC results for the three groups on the Day 9 in the pOVAR test (tilt angle: 10°, 20°, 30°, 40° at 0.2 Hz). **C**, Traces show horizontal eye velocity (tilt angle: 30°, 0.2 Hz) for control, mid-dose (2 mg/g), and high-dose (4 mg/g) groups. **D**, The H-FPN frequency for three groups on the Day 9 of the pOVAR test (tilt angle: 30° at 0.2, 0.3, 0.4 Hz). **E**, The horizontal mean slow-phase velocity for three groups on the Day 9 of the pOVAR test (tilt angle: 30°, 40° at 0.2 Hz in CW direction). CW is a positive direction, so the bias component is negative. **F**, Traces display horizontal eye displacement and horizontal eye velocity in control and baclofen-treated groups. **G**, The ratio of H-FPN frequency post-baclofen injection compared with pre-injection (tilt angle: 30° at 0.2 Hz). After administration, the H-FPN frequency significantly decreased in the high-dose group (10 mg/kg), while no significant change was observed in the control group. **H**, Traces display vertical eye displacement in control and baclofen-treated groups. **I**, pOVAR V-SMC results in the three groups (tilt angle: 30° at 0.2, 0.3, 0.4 Hz). Baclofen injection had little impact on SMC during pOVAR test (* $p < 0.05$, ** $p < 0.01$, *** $p < 0.001$, **** $p < 0.0001$).

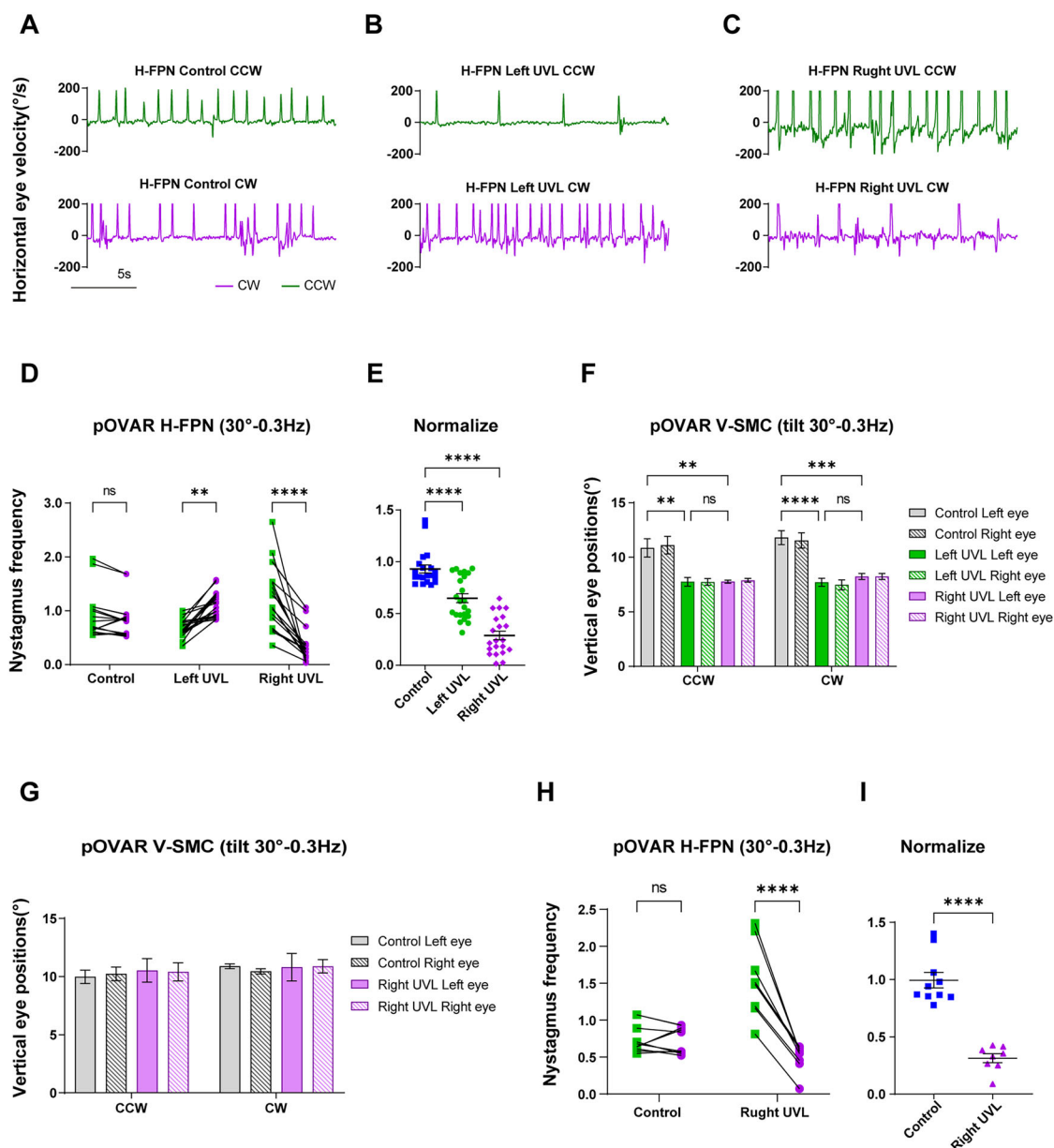


Figure 3. Dynamic characteristic of VOR in control, UVL, and unilateral SCD mice. Means \pm standard error of mean (SEM) is shown in the results. **A–C,** Traces show the horizontal eye velocity in healthy (control), left-UVL, and right-UVL mice during pOVAR test in both CCW and CW direction. **D,** The H-FPN frequency in all groups during CCW and CW direction rotation (tilt angle: 30° at 0.3 Hz). **E,** Normalize the data of graph (D). Control, CW/CCW; left-UVL, CCW/CW; right-UVL, CW/CCW. **F,** Left and right eye V-SMC across all groups during CCW and CW stimulation (tilt angle: 30° at 0.3 Hz). **G,** Similar to F, V-SMC in control and L-SCD groups. **H, I,** Similar to D and E in right-UVL mice caused by L-SCD. After drilling a hole in the middle of LSC, the outflow endolymphatic fluid was absorbed with sterile cotton, after which the wound was sutured. The V-SMC and H-FPN frequency under other stimulus conditions are shown in Extended Data Figure 3-1 ($p < 0.05$, $**p < 0.01$, $***p < 0.001$, $****p < 0.0001$).

OVAR test (Fig. 5J; Extended Data Fig. 5-1E, two-way ANOVA). These results indicated that the input from the SCCs may contribute to the generation of the H-FPN during pOVAR and OVAR tests.

Discussion

The signals from SCCs can influence the generation of FPN in mouse OVAR test

During the pOVAR test, nystagmus is induced as long as rotation persists, consisting of SMC modulated at the same frequency as the stimulus and bias component related to horizontal eye velocity (Kushiro et al., 2002). The SMC exhibits a high degree of consistency with vestibular stimulation. V-SMC reflects changes in head orientation relative to gravity, whereas H-SMC reflects the effect of translational acceleration acting on the head. It is widely accepted that the bias

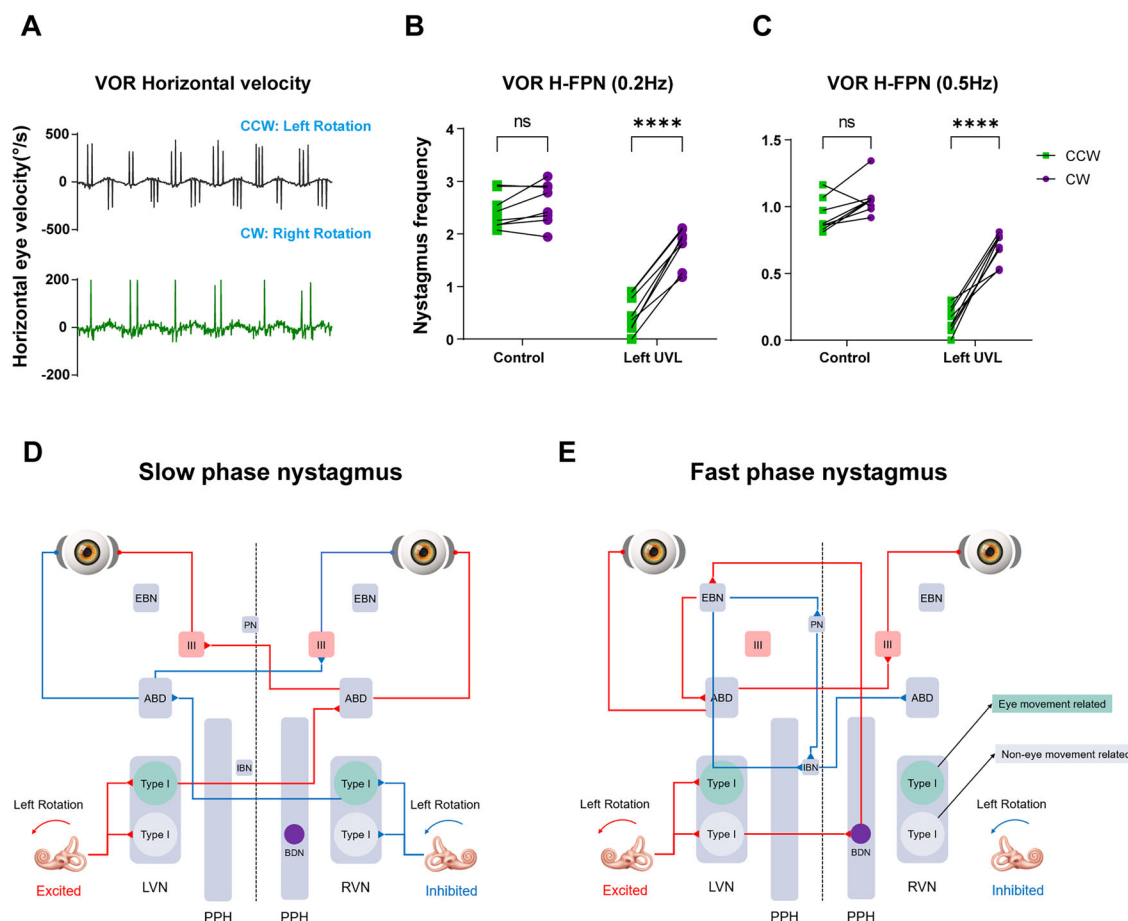


Figure 4. Illustration of the neural pathway for slow-phase and fast-phase eye movement in aVOR during leftward head rotation. **A**, Traces show the horizontal eye velocity in control and left-UVL mice during aVOR test. **B**, **C**, the H-FPN frequency during aVOR test (0.2, 0.5 Hz) in control and left-UVL groups. **D**, Neural pathway involved in SPN generation. **E**, Neural pathway involved in FPN generation. LVN, left vestibular nucleus; PPH, prepositus hypoglossi; BDN, burster driver neuron; EBN, excitatory burst neuron; IBN, inhibitory burst neuron; PN, pause neuron; ABD, abducens neuron; III, ocular motor nucleus.

component established by VSM to compensate for head angular velocity in the OVAR test originates from the activation of the otolith organs (Darlot et al., 1988). The central VSM, acting as a multisensory rotational estimator, integrates rotational information through its internal rotational sensors to decompose ambiguous otolith signals into tilt and translation components. As the SCCs signals decay, the emergence of bias allows the VSM to maintain a constant velocity output, thereby minimizing otolith prediction errors to the greatest extent (Laurens and Angelaki, 2011). In practice, the bias component opposite to head movement is equivalent to the H-FPN in the same direction as the head, due to the eye movements within the orbit. Consequently, the H-FPN frequency accurately reflects the magnitude of the bias component. From a data processing perspective, calculating the bias component typically introduces larger errors compared with extracting FPN components.

However, *zpld1*^{-/-} mice with intact otolith function exhibit no FPN component during the OVAR test, indicating that the SCCs may also contribute to the generation of FPN. This hypothesis is further supported by results from mice with bilateral L-SCD, which corroborate this perspective. Mice with only unilateral semicircular canal injury also exhibited abnormalities in the FPN. Additionally, *Otop1*^{tit/tit} mice exhibit a normal vestibular time constant, indicating that both SCCs and VSM functions are intact (Khan et al., 2019). At the onset of OVAR, the SCCs are activated, leading to the appearance of “jerk” nystagmus. As the rotation continues, the SCCs signals gradually decay to resting levels (Raphan et al., 1983), and in the absence of otolith input, both SMC and FPN disappear. The SCCs signals serve as the primary input to the central VSM rotational velocity estimator. Any form of SCC dysfunction can impair the central establishment of head angular velocity (Denise et al., 1996). Consequently, bilateral semicircular canal damage may result in the loss of the VSM’s ability to estimate angular head velocity. The emergence of the bias component or FPN serves as a compensatory mechanism for the decline in SCC input, resulting from internal tilt estimator feedback to the VSM. Crucially, through this feedback loop, the central nervous system can convert the continuous otolithic signals into a constant angular velocity (Fig. 6, $k_f \text{GIA} \times \text{G}$; Laurens and Angelaki, 2011). In summary, the generation of FPN in the OVAR model requires continuous

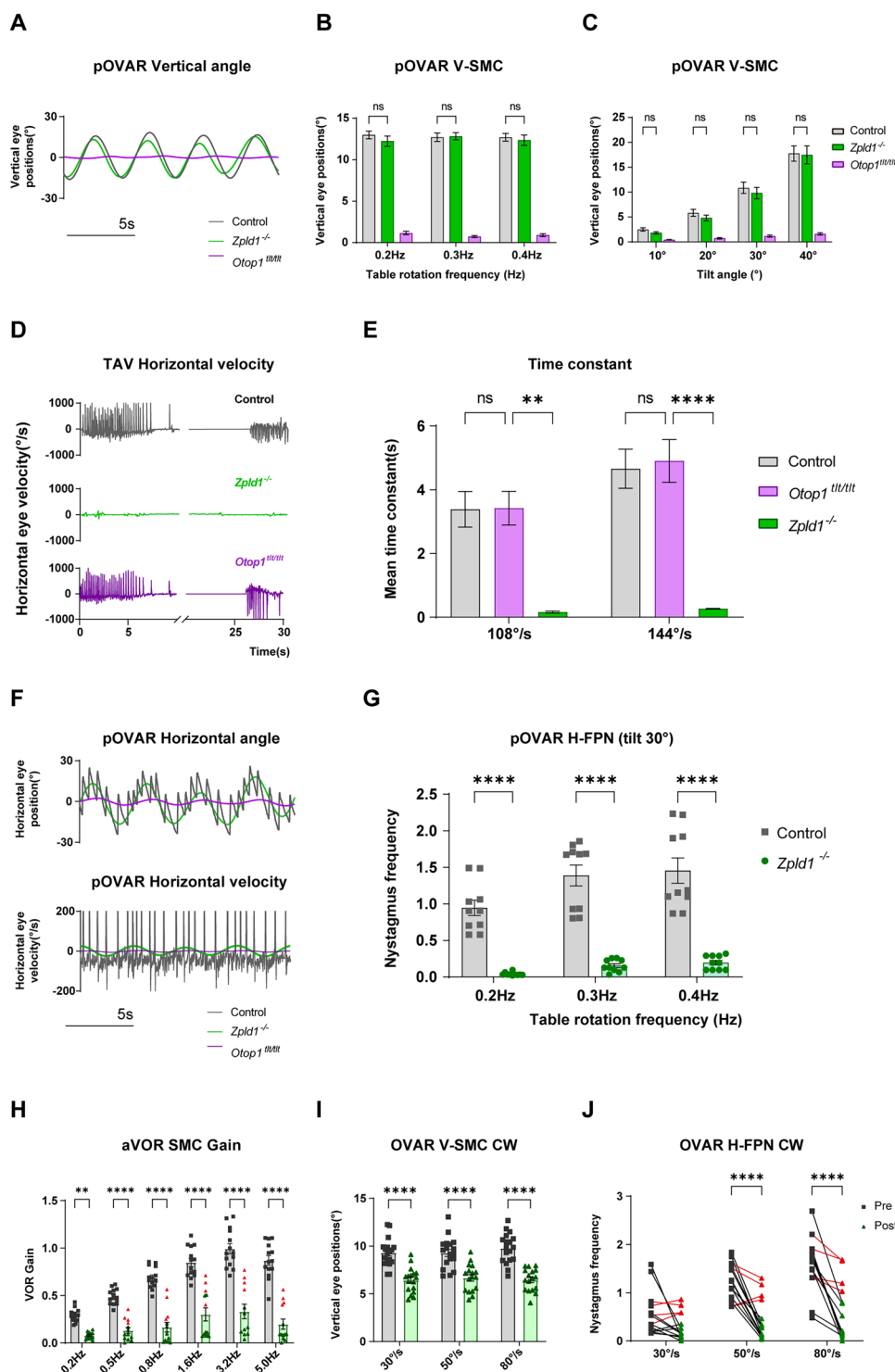


Figure 5. Vestibular function test in *Zpld1* and *Otop1* mutant mice. Means \pm standard error of mean (SEM) is shown in the results. **A**, Traces show vertical eye displacement during pOVAR test in control, *Zpld1*^{-/-} and *Otop1*^{tit/tit} mice. **B**, V-SMC of control, *Zpld1*^{-/-} and *Otop1*^{tit/tit} mice during pOVAR test (tilt angle: 30° at 0.2, 0.3, 0.4 Hz). **C**, V-SMC (tilt angle: 10°, 20°, 30°, 40° at 0.2 Hz). The V-SMC of control, *Zpld1*^{-/-} and *Otop1*^{tit/tit} mice during test (tilt angle: 20° at 0.2, 0.3, 0.4 Hz) are shown in Extended Data Figure 4-1B. **D**, Traces show horizontal eye velocity during TAV test in control, *Zpld1*^{-/-} and *Otop1*^{tit/tit} mice. The stimulus paradigm of the TAV model is shown in Extended Data Figure 4-1F. **E**, represent the vestibular time constant in TAV test. **F**, Traces show horizontal eye displacement and horizontal eye velocity during pOVAR test in control, *Zpld1*^{-/-} and *Otop1*^{tit/tit} mice. **G**, The H-FPN frequency during pOVAR test in control and *Zpld1*^{-/-} mice (tilt angle: 30° at 0.2, 0.3, 0.4 Hz), and the results in other stimulus condition (tilt angle: 20° at 0.2, 0.3, 0.4 Hz) are shown in Extended Data Figure 4-1A. **H**, **I**, represent the SMC information of VOR and OVAR test in mice with bilateral L-SCD. **J**, The H-FPN frequency during OVAR test in CCW direction. The V-SMC gain and H-FPN frequency during OVAR test in CCW direction are shown in Extended Data Figure 4-1C-E (* $p < 0.05$, ** $p < 0.01$, *** $p < 0.001$, **** $p < 0.0001$).

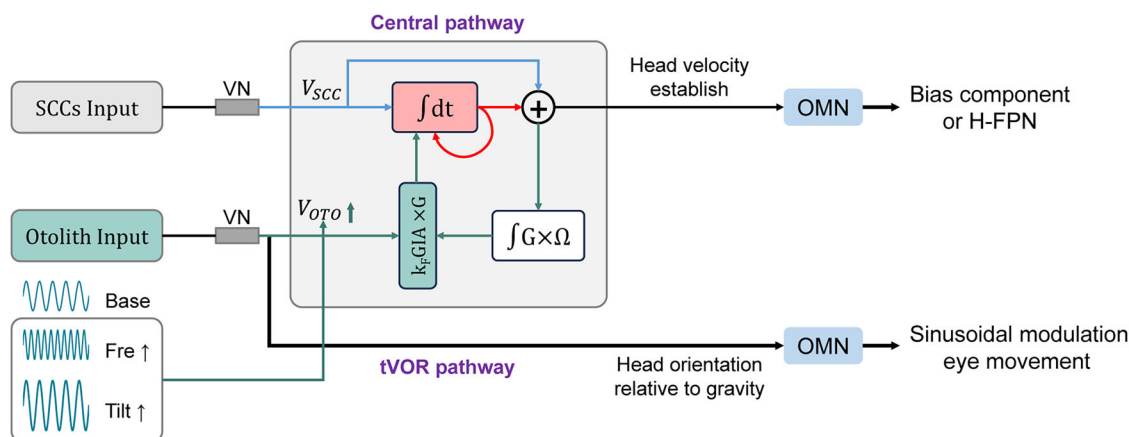


Figure 6. Schematic diagram of direct and indirect pathways for SCCs and otolith information in the OVAR test. VN, vestibular nucleus; OMN, ocular motor neurons; V_{SCC} , SCCs velocity signal; V_{OTO} , otolith signal; GIA, gravito-inertial acceleration; k_F , coefficient; Ω , angular velocity vector; G , gravity vector; \times , vectorial cross-product; $\int G \times \Omega$, tilt estimator.

otolithic signals, while the VSM converts periodic oscillatory otolithic inputs into a sustained FPN (bias component). Otolith signals are transduced into V-SMC via the orientation mechanisms. Additionally, increasing the rotational frequency or the tilt angle both lead to an increase in V_{OTO} , ultimately resulting in an increase in H-FPN frequency.

The FPN effectively identifies a variety of subtle vestibular dysfunctions

The generation of FPN in OVAR relies on peripheral otolith input and central VSM, implying that abnormalities in FPN may indicate dysfunctions in either the peripheral or central pathways. If the injury affects only the central pathway, the FPN is affected while the SMC remains relatively normal, as observed following baclofen injections (Shimizu et al., 2016). However, both the FPN and SMC can be affected if the injury involves peripheral receptors, such as in the case of IDPN administration or UVL induced by gentamicin injections.

In this study, the bias in FPN exhibits high sensitivity for detecting unilateral vestibular impairment, even after vestibular compensation has occurred. This bias is attributed to asymmetric oscillatory signals from the peripheral labyrinth being transmitted to the central velocity storage network. In clinical practice, the diagnosis of central vestibular lesions using head-shaking-induced nystagmus relies on a similar mechanism (Choi and Kim, 2009). Some studies have shown that the brain optimizes the velocity storage integration network based on the signal-to-noise ratio (SNR) of peripheral vestibular input (Madhani et al., 2022). Even following central compensation after peripheral damage, the noise inherent in lesioned afferents and vestibular nuclei persists, leading to a reduction in the SNR of ipsilateral input signals. This reduction results in a decreased vestibular time constant and diminished capacity of central VSM to reconstruct head angular velocity. Consequently, during the OVAR test, there is a reduction in either the bias component or the FPN.

Summary

In this study, we investigated the contribution of different vestibular structures to the generation of FPN during the OVAR test in mice. Our findings align with previous research on primates, demonstrating that the generation of FPN in the OVAR test requires not only otolithic signals but also substantial input from the SCCs. The SCCs provide the primary input to the neural estimator of the rotational velocity in the central VSM, and the reconstruction of angular velocity using otolith signals by the central nervous system also depends on the participation of this estimator. Consequently, SCC input may modify this rotation estimator to regulate the generation of FPN during OVAR and explain the FPN bias following UVL. Additionally, the FPN frequency during OVAR was extracted, facilitating the effective identification of subtle vestibular dysfunctions, particularly those undetectable using traditional SMC assessments. For instance, the central pathways involving the VOR, such as the vestibulocerebellum, as well as UVL, align with previous findings (Gilchrist et al., 2003; Fig. 4C) and exhibit a more pronounced contrast.

References

- Angelaki DE, Hess BJ (1996) Three-dimensional organization of otolith-ocular reflexes in rhesus monkeys. I. Linear acceleration responses during off-vertical axis rotation. *J Neurophysiol* 75:2405–2424.
- Armstrong PA, Wood SJ, Shimizu N, Kuster K, Perachio A, Makishima T (2015) Preserved otolith organ function in caspase-3-deficient mice with impaired horizontal semicircular canal function. *Exp Brain Res* 233:1825–1835.
- Behrens F, Weiss LR (1992) An algorithm separating saccadic from nonsaccadic eye movements automatically by use of the acceleration signal. *Vision Res* 32:889–893.

- Beraneck M, Cullen KE (2007) Activity of vestibular nuclei neurons during vestibular and optokinetic stimulation in the alert mouse. *J Neurophysiol* 98:1549–1565.
- Beraneck M, McKee JL, Aleisa M, Cullen KE (2008) Asymmetric recovery in cerebellar-deficient mice following unilateral labyrinthectomy. *J Neurophysiol* 100:945–958.
- Brettler SC, Rude SA, Quinn KJ, Killian JE, Schweitzer EC, Baker JF (2000) The effect of gravity on the horizontal and vertical vestibulo-ocular reflex in the rat. *Exp Brain Res* 132:434–444.
- Burns JC, Stone JS (2017) Development and regeneration of vestibular hair cells in mammals. *Semin Cell Dev Biol* 65:96–105.
- Choi KD, Kim JS (2009) Head-shaking nystagmus in central vestibulopathies. *Ann N Y Acad Sci* 1164:338–343.
- Choi KD, Oh SY, Park SH, Kim JH, Koo JW, Kim JS (2007) Head-shaking nystagmus in lateral medullary infarction: patterns and possible mechanisms. *Neurology* 68:1337–1344.
- Cohen B, Dai M, Yakushin SB, Raphan T (2008) Baclofen, motion sickness susceptibility and the neural basis for velocity storage. *Prog Brain Res* 171:543–553.
- Curthoys IS (2002) Generation of the quick phase of horizontal vestibular nystagmus. *Exp Brain Res* 143:397–405.
- Dai M, Raphan T, Cohen B (2006) Effects of baclofen on the angular vestibulo-ocular reflex. *Exp Brain Res* 171:262–271.
- Darlot C, Denise P, Droulez J, Cohen B, Berthoz A (1988) Eye movements induced by off-vertical axis rotation (OVAR) at small angles of tilt. *Exp Brain Res* 73:91–105.
- Denise P, Darlot C, Ignatiew-Charles P, Toupet M (1996) Unilateral peripheral semicircular canal lesion and off-vertical axis rotation. *Acta Otolaryngol* 116:361–367.
- Ebenezer IS, Prabhaker M (2007) The effects of intraperitoneal administration of the GABA(B) receptor agonist baclofen on food intake in CFLP and C57BL/6 mice. *Eur J Pharmacol* 569:90–93.
- Ebisawa Y, Minamitani H, Mori Y, Takase M (1988) New methods for removing saccades in analysis of smooth pursuit eye movement. *Biol Cybern* 60:111–119.
- Fetter M (2007) Vestibulo-ocular reflex. *Dev Ophthalmol* 40:35–51.
- Fetter M (2016) Acute unilateral loss of vestibular function. *Handb Clin Neurol* 137:219–229.
- Furman JM (2010) Rotational testing: background, technique and interpretation. *Handb Clin Neurophysiol* 9:141–149.
- Gao Y, Kamogashira T, Fujimoto C, Iwasaki S, Yamasoba T (2022) Beneficial effects of time-restricted feeding on gentamicin cytotoxicity in mouse cochlea and vestibular organs. *Laryngoscope Invest Otolaryngol* 7:530–539.
- Gilchrist DP, Cartwright AD, Burgess AM, Curthoys IS (2003) Behavioural characteristics of the quick phase of vestibular nystagmus before and after unilateral labyrinthectomy in guinea pig. *Exp Brain Res* 149:289–298.
- Guo JY, Liu YY, Qu TF, Peng Z, Xie J, Wang GP, Gong SS (2017) Cochleovestibular gene transfer in neonatal mice by canalostomy. *Neuroreport* 28:682–688.
- Guo JY, He L, Qu TF, Liu YY, Liu K, Wang GP, Gong SS (2018) Canalostomy as a surgical approach to local drug delivery into the inner ears of adult and neonatal mice. *J Vis Exp* 135:e57351.
- Hubner PP, Khan SI, Migliaccio AA (2017) The mammalian efferent vestibular system plays a crucial role in vestibulo-ocular reflex compensation after unilateral labyrinthectomy. *J Neurophysiol* 117:1553–1568.
- Hupfeld KE, et al. (2022) Brain and behavioral evidence for reweighting of vestibular inputs with long-duration spaceflight. *Cereb Cortex* 32:755–769.
- Hurle B, Ignatova E, Massironi SM, Mashimo T, Rios X, Thalmann I, Thalmann R, Ornitz DM (2003) Non-syndromic vestibular disorder with otoconial agenesis in tilted/mergulador mice caused by mutations in otopenin 1. *Hum Mol Genet* 12:777–789.
- Kanayama R, Kato I, Nakamura T, Koike Y (1987) The fast-phase velocity of optokinetic nystagmus in central nervous system disorders. *Acta Otolaryngol* 104:392–399.
- Katsarkas A, Galiana H, Smith H (1991) Does the vestibulo-ocular reflex (VOR) merit redefinition? *Otolaryngol Head Neck Surg* 105:633–640.
- Kaufman GD (2002) Video-oculography in the gerbil. *Brain Res* 958:472–487.
- Khan HA, Alhomida AS, Arif IA (2009) Neurovestibular toxicities of acrylonitrile and iminodipropionitrile in rats: a comparative evaluation of putative mechanisms and target sites. *Toxicol Sci* 109:124–131.
- Khan SI, Della Santina CC, Migliaccio AA (2019) Angular vestibuloocular reflex responses in Otop1 mice. I. Otolith sensor input is essential for gravity context-specific adaptation. *J Neurophysiol* 121:2291–2299.
- Khan SI, Hubner PP, Brichta AM, Migliaccio AA (2022) Vestibulo-ocular reflex short-term adaptation is halved after compensation for unilateral labyrinthectomy. *J Assoc Res Otolaryngol* 23:457–466.
- Kim SH, Lee SY, Kim JS, Koo JW (2021) Parameters of off-vertical axis rotation in unilateral and bilateral vestibulopathy and their correlation with vestibular evoked myogenic potentials. *J Clin Med* 10:4.
- Kushiro K, Dai M, Kunin M, Yakushin SB, Cohen B, Raphan T (2002) Compensatory and orienting eye movements induced by off-vertical axis rotation (OVAR) in monkeys. *J Neurophysiol* 88:2445–2462.
- Laurens J, Angelaki DE (2011) The functional significance of velocity storage and its dependence on gravity. *Exp Brain Res* 210:407–422.
- Madhani A, Lewis RF, Karmali F (2022) How peripheral vestibular damage affects velocity storage: a causative explanation. *J Assoc Res Otolaryngol* 23:551–566.
- Maruta J, Simpson JL, Raphan T, Cohen B (2001) Orienting otolith-ocular reflexes in the rabbit during static and dynamic tilts and off-vertical axis rotation. *Vision Res* 41:3255–3270.
- Ng AKT, Chan LKY, Lau HYK (2020) A study of cybersickness and sensory conflict theory using a motion-coupled virtual reality system. *Displays* 61:101922.
- Nist-Lund CA, et al. (2019) Improved TMC1 gene therapy restores hearing and balance in mice with genetic inner ear disorders. *Nat Commun* 10:236.
- Ono K, et al. (2020) Retinoic acid degradation shapes zonal development of vestibular organs and sensitivity to transient linear accelerations. *Nat Commun* 11:63.
- Osoba MY, Rao AK, Agrawal SK, Lalwani AK (2019) Balance and gait in the elderly: a contemporary review. *Laryngoscope Invest Otolaryngol* 4:143–153.
- Ranjbaran M, Smith HL, Galiana HL (2016) Automatic classification of the vestibulo-ocular reflex nystagmus: integration of data clustering and system identification. *IEEE Trans Biomed Eng* 63:850–858.
- Raphan T, Waespe W, Cohen B (1983) Labyrinthine activation during rotation about axes tilted from the vertical. *Adv Otorhinolaryngol* 30:50–53.
- Sadeghi SG, Minor LB, Cullen KE (2011) Multimodal integration after unilateral labyrinthine lesion: single vestibular nuclei neuron responses and implications for postural compensation. *J Neurophysiol* 105:661–673.
- Shimizu N, Wood S, Kushiro K, Yanai S, Perachio A, Makishima T (2015) Dynamic characteristics of otolith ocular response during counter rotation about dual yaw axes in mice. *Neuroscience* 285:204–214.
- Shimizu N, Wood S, Kushiro K, Perachio A, Makishima T (2016) The role of GABAB receptors in the vestibular oculomotor system in mice. *Behav Brain Res* 302:152–159.
- Simon F, Tissir F, Michel V, Lahlou G, Deans M, Beraneck M (2021) Implication of vestibular hair cell loss of planar polarity for the canal and otolith-dependent vestibulo-ocular reflexes in Celsr1(-/-) mice. *Front Neurosci* 15:750596.
- Vijayakumar S, Jones SM, Jones TA, Tian C, Johnson KR (2019) Spontaneous mutations of the Zpld1 gene in mice cause

- semicircular canal dysfunction but do not impair gravity receptor or hearing functions. *Sci Rep* 9:12430.
- Wang C, Tian J, Liang P, Sun F (2005) Diazepam-induced changes of optokinetic nystagmus fast phase. *Exp Brain Res* 167:446–450.
- Wilkerson BA, Artoni F, Lea C, Ritchie K, Ray CA, Bermingham-McDonogh O (2018) Effects of 3,3'-iminodipropionitrile on hair cell numbers in cristae of CBA/CaJ and C57BL/6J mice. *J Assoc Res Otolaryngol* 19:483–491.
- Yang X, Sun P, Wu JP, Jiang W, Vai MI, Pun SH, Peng C, Chen F (2020) Nondestructive and objective assessment of the vestibular function in rodent models: a review. *Neurosci Lett* 717:134608.
- Zeng S, et al. (2020) Toxic effects of 3,3'-iminodipropionitrile on vestibular system in adult C57BL/6J mice in vivo. *Neural Plast* 2020:1823454.